Correlation between functional and ultrastructural substrate in Brugada syndrome

Pablo E. Tauber, MD,[*†] Virginia Mansilla, MD,[*] Guillermo Mercau, MD,[*] Felix Albano, MD,[†] Ricardo R. Corbalán,[*] Sara S. Sánchez, PhD,[‡] Stella M. Honoré, PhD[‡]

From the [*]Electrophysiology Division, Model Heart Center, San Miguel de Tucumán, Argentina, [†]Unit of Arrhythmias and Electrophysiology, ZJS Hospital Health Center, San Miguel de Tucumán, Argentina and [‡]Departamento Biología del Desarrollo, INSIBIO (Consejo Nacional de Investigaciones Científicas y Técnicas-Universidad Nacional de Tucumán) (CONICET-UNT) San Miguel de Tucumán, Argentina.

Introduction

Brugada syndrome (BS) was reported for the first time in 1992 and is associated with an ST-segment elevation in the right precordial leads in the absence of any demonstrable structural heart disease, as well as with sudden cardiac death due to ventricular fibrillation (VF).[1] A patent type 1 electrocardiogram (ECG) is diagnostic of BS and is characterized by a coved ST-segment elevation of ≥ 2 mm followed by a negative T wave in >1 right precordial lead (V1 to V3) in the presence or absence of a sodium channel–blocking agent, and in conjunction with 1 of the following: documented VF, polymorphic ventricular tachycardia (VT), a family history of sudden cardiac death at <45 years of age, coved-type ECGs in family members, inducibility of VT/VF with programmed electrical stimulation, syncope, or nocturnal agonal respiration.[2] An autosomal dominant disease with incomplete penetrance, BS has been linked to mutations in *SCN5A*, the gene encoding the alpha subunit of the cardiac sodium channel. Still, *SCN5A* mutations have been reported in only approximately 20% of patients with BS diagnosed on the basis of clinical criteria, suggesting that other genetic defects or other disease mechanisms may give rise to this clinical picture.[3]

Noninvasive ECG imaging reveals that the abnormal electrophysiological substrate is localized in the right ventricular outflow tract (RVOT). Both abnormal repolarization and abnormal conduction are present in the substrate.[2,3]

KEYWORDS Brugada syndrome; Biopsy; Right ventricular outflow tract; Radiofrequency catheter ablation; Electrocardiography; Electrophysiology study

(Heart Rhythm Case Reports 2016;2:211–216)

S. S. S. and S. M. H. are career investigators of CONICET (Argentina). Sources of Funding: This work was supported by grants from Consejo Nacional de Investigaciones Científicas y Técnicas (CONICET) PIP 112 201101 00529 and Agencia Nacional de Promoción Científica y Tecnológica (ANPCyT) PICT 2013–1949. Conflict of Interest: The authors declare that there are no conflicts of interest. Codes pertaining to the article: Etiology [5], Treatment [22], Diagnosis testing [106] [33] **Address reprint requests and correspondence:** Dr Pablo Tauber, Laprida 544, San Miguel de Tucumán, Argentina, 4000. E-mail address: pablotauber@gmail.com.

The presence of structural cardiac disease as part of the phenotype of BS has been suggested repeatedly but never demonstrated conclusively. The relationships in BS between the clinical manifestations, the presence of SCN5A gene mutations, and structural heart disease are highly complex. Frustaci et al[4] used an optical microscope to observe hypertrophy and vacuolization of cardiac myocytes in endomyocardial biopsies of the septoapical region of the right ventricle from 3 patients. This study suggests that right ventricular biopsy is the more sensitive approach to identifying structural heart disease in patients with a phenotype of BS. In this regard, more studies need to be done to clarify the mechanistic links between the electrical substrate in BS and the presence of a structural substrate.

The aim of the present study was to investigate whether concealed cardiac abnormalities are present in a patient diagnosed with BS and whether there is a correlation between functional analysis and possible ultrastructural alterations. We report the results of an endomyocardial biopsy, guided by voltage and electroanatomic mapping of the RVOT, with transmission electron microscopy (TEM) analysis and the correlation of these results with clinical, electrophysiological, and ECG findings. The present results shed new light on the pathophysiology of the disease and may help to account for its arrhythmic manifestations.

Case report

A 38-year-old white woman, a nurse who experienced frequent syncopal episodes, was admitted to our hospital in April 2014. At admission, a clinical and family history was collected, and the patient underwent physical examination and noninvasive studies that included 2-dimensional echocardiography, tilt test, computed tomography of the brain, electroencephalography, Holter monitoring, human immunodeficiency virus testing, laboratory testing, myocardial perfusion scan, and cardiac magnetic resonance imaging. The study protocol was approved by the institutional ethics committee. Systemic diseases, Chagas disease, drug abuse,

http://dx.doi.org/10.1016/j.hrcr.2015.12.001

KEY TEACHING POINTS

- Abnormal electrophysiological substrate is localized in the right ventricular outflow tract. Both abnormal depolarization and abnormal conduction are present in the substrate.
- We investigated the hidden heart defects and the correlation between functional analysis and ultrastructural alterations present in a patient with Brugada syndrome.
- We report the endomyocardial biopsy, guided for voltage map of the right ventricular outflow tract, with transmission electron microscopy analysis and the correlation with clinical, electrophysiological, and electrocardiographic findings.
- We report the cell damage and death, progressively from a peripheral to a central, very low-voltage area.
- We recognize 3 functional and ultrastructural areas on the substrate: a central area of very low voltage, another peripheral area of intermediate voltage, and finally a more peripheral area of normal features.
- Guided by systolic voltage electrograms (EGMs) map and diastolic bipolar EGMs, we identify areas that contained low-amplitude late potentials, middiastolic EGMs, and presystolic Purkinje-type potentials. All these areas were targets for ablation.

electrolyte imbalance, and echocardiographic abnormalities of the heart valves, the right and left ventricular dimensions, and contractility were excluded. The patient had no family history of BS or sudden cardiac death, but we found an asymptomatic 17-year-old daughter with an induced patent type 1 ECG. The diagnosis of BS was suspected after we documented a patent type 2 ECG with saddleback appearance, with a high takeoff ST-segment elevation of >2 mm followed by a biphasic T wave in either lead V1 or lead V2 in the second intercostal space (ICS) and we also noted the presence of end-QRS slurs in the DI and aVL leads, with a J-point peak of ≥ 0.2 mV and ST segment descending in the DI lead and horizontal in the aVL lead, corresponding to an early repolarization. BS was definitively diagnosed when the patent type 2 (saddleback) ECG was converted to type 1 after challenge with a sodium-channel blocker (flecainide 400 mg, orally), in precordial lead V1 to V3 in the second ICS, which was associated with a final R wave of aVR of 3 mv, prolonged QRS duration in V2 of 150 milliseconds (Figure 1), and documented VF induced with programmed electrical stimulation. The patient did not accept an implantable cardiac defibrillator.

After obtaining written informed consent, we performed an electrophysiological study, electroanatomic and voltage mapping, endomyocardial biopsy, and catheter ablation procedure. The study was conducted with the patient in a fasting, drug-free, and sedated state. Under fluoroscopic guidance, a 6F quadripolar catheter (St Jude Medical, St Paul, MN) and a 7F deflectable decapolar catheter (Livewire TC, St Jude Medical) were introduced into the His bundle region and coronary sinus, respectively, via the femoral veins. Detailed mapping was performed in the RVOT using a 7F Safire quadripolar ablation catheter with an 8-mm distal electrode, an embedded thermistor, and a deflectable tip (St. Jude Medical). Endocardial potentials were filtered to recording frequencies of 30 to 500 Hz and recorded on a computer system (Feas Electrónica AR, Córdoba, Argentina). During the procedure, the baseline interval AH was 110 milliseconds, HV-DI was 60 milliseconds, HV-V2 was 40 milliseconds, QRS duration in DII was 90 milliseconds, and QRS duration in V2 was 150 milliseconds (Figure 2A). The protocol of programmed electrical stimulation from RVOT was performed (2 drive and ≤ 3 extrastimuli from RVOT). An S1-S2 interval was applied after 8 beats of drive pacing at basic cycle lengths of 600 to 400 milliseconds. The S1-S2 interval was decreased in 20-millisecond steps until the effective refractory period of the right ventricle, which was 180 milliseconds, was reached. During a stimulation in which the S1S1 value was 600 milliseconds, the S1-S2 interval was 240 milliseconds, and the S2-S3 interval was 200 milliseconds, we induced VF that lasted >10 seconds and required an electric shock. Premature ventricular complexes (PVCs) with a left bundle branch block morphology, inferior axis, transition of $>$V3, and transitional zone index of 1 occurred repetitively before episodes of spontaneous VT from the RVOT area and preceded diastolic electrograms (EGMs) (Figures 2B and 2C). Electroanatomic and voltage mapping of the right ventricular and RVOT endocardium was performed with the EnSite NavX system (St. Jude Medical) (Figure 2D). Bipolar signals were filtered at 30 to 400Hz and displayed at 100 to 200 mm/s. We defined 3 zones according to the voltage amplitude of systolic EGMs: a central very low-voltage zone of <0.5mV, a peripheral low-voltage zone of 0.5 to 1.5mV, and a normal voltage zone of >1.5 mV (Figures 2D and 3). After accessing the right internal jugular vein with a 7.2F 45-cm deflectable sheath catheter (Attain deflectable catheter delivery system, Medtronic, Minneapolis, MN), we connected a bioptome [Jawz Endomyocardical biopsy forceps (Argon Medical, Plano, TX), 6F, length 50 cm] to the NavX system and obtained endomyocardial biopsies of the 3 previously defined areas, guiding by electroanatomic and voltage maps. Samples were fixed in 4% glutaraldehyde and 0.1% sodium phosphate (pH 7.4) for the TEM study, as was described previously.[5] Guided by voltage EGMs map systolic, electroanatomic map, and bipolar EGMs diastolic, we identified areas that contained low-amplitude late potentials, middiastolic EGMs, and presystolic Purkinje-type potentials of low amplitude and high frequency preceding the QRS for 20 or

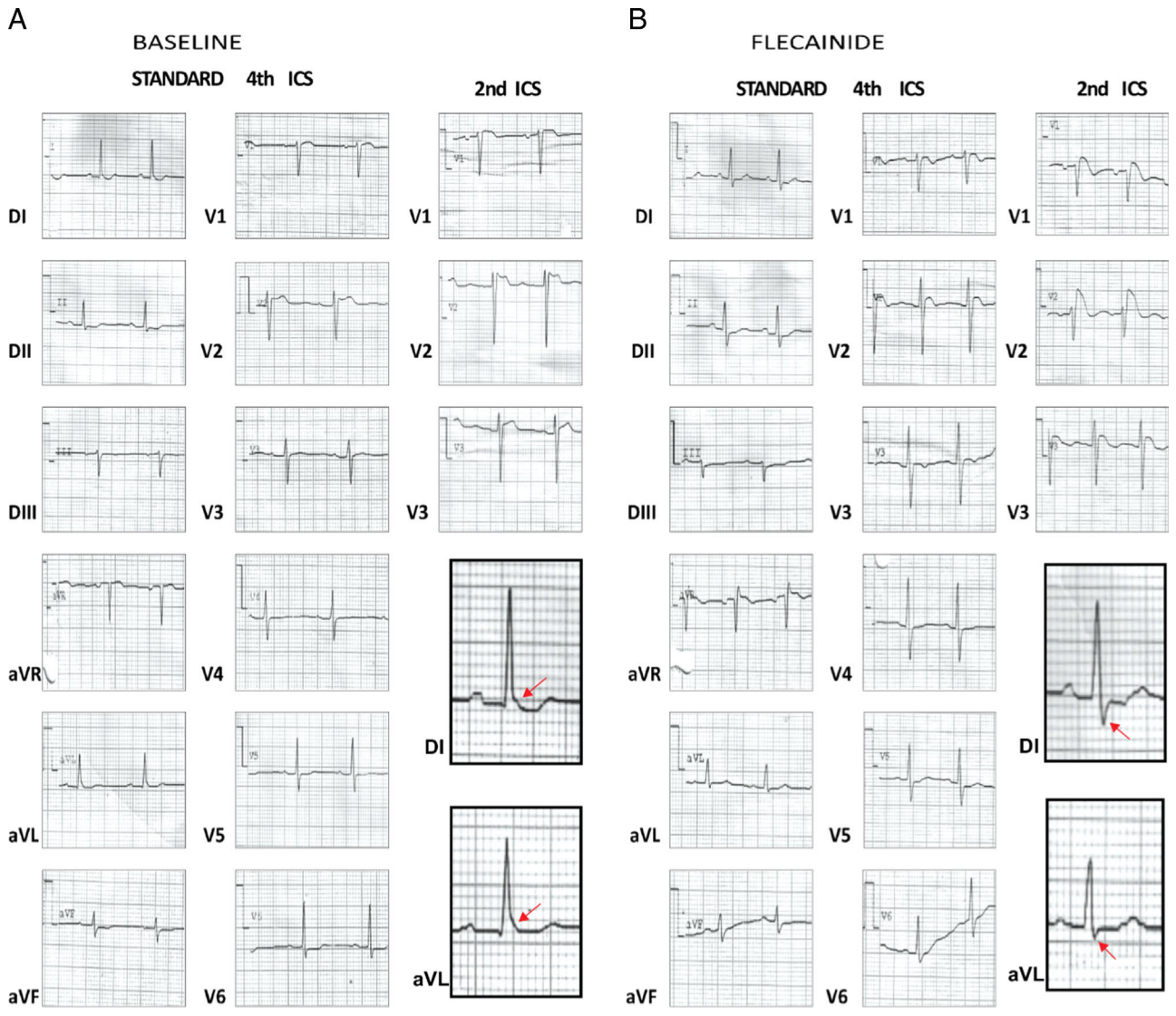

Figure 1 **A:** Twelve-lead electrocardiogram (ECG) tracings baseline: patent type 2 ECG (not diagnostic) displaying a PR interval of 200 milliseconds, QRS axis of 0°, QRS duration in V2 [fourth intercostal space (ICS)] of 120 milliseconds, QT/QTc of 360/383 milliseconds, the presence of an end-QRS slur with a descending ST segment in DI and horizontal in aVL, and saddleback-type ST-segment elevation observed in V2 (second ICS). Shift of right precordial leads in second higher ICSs does not reveal a type 1 patent ECG, but an increased saddleback-type ST-segment elevation is observed in V2. Note the presence of the end-QRS slur in DI and aVL, with a J-point peak $\geq$0.2 mV and descending ST segment in DI and horizontal in aVL (red arrows). **B:** Twelve-lead ECGs after oral administration of 400 mg of flecainide: In the third hour, the type 2 ECG is converted to the diagnostic type 1 patent ECG, which consists of a coved-type ST-segment elevation, observed in V2 of the standard 12-lead ECG (fourth ICS) and in V1, V2, and V3 recorded from the second ICS. Depolarization abnormalities are present as a prolonged PR interval of 210 milliseconds, QRS axis +8°, prolonged QRS duration in V2 of 150 milliseconds, and a high final R wave in aVR of 3 mm, consistent with right end conduction delay. Repolarization disorder can also be seen, with a prolonged QT/QTc interval of 420/481 milliseconds. Note the disappearance of the end-QRS slur in DI and aVL and the appearance of S waves and leveling ST segment (red arrows).

30 milliseconds. All these areas were targets for ablation by radiofrequency application through a team of IBIS (Irvine Biomedical, Irvine, CA) with a 50-W power setting, a temperature of 60°C, and a total duration of 60 seconds per application to confirm the disappearance of the diastolic EGMs and PVCs. Then, the same stimulation protocol used previously to induce VF was applied. Until the ventricular refractory period, VF was not induced.

The patient was followed up monthly with physical examination, resting ECG, Holter monitoring, and 2-dimensional echocardiogram. The patient has not experienced symptoms or arrhythmia, and the ECG has shown no evidence of a BS pattern during follow-up as of the time of this publication.

Discussion

Some studies have considered BS a heart disease characterized by functional electrical abnormalities mainly at the RVOT, without evident morphological abnormalities. The presence of unfractionated systolic EGMs of low voltage in the endocardium has been reported,[6] although the researchers noted the greater magnitude of these potentials, which were targets for ablation, in the epicardium, where they were

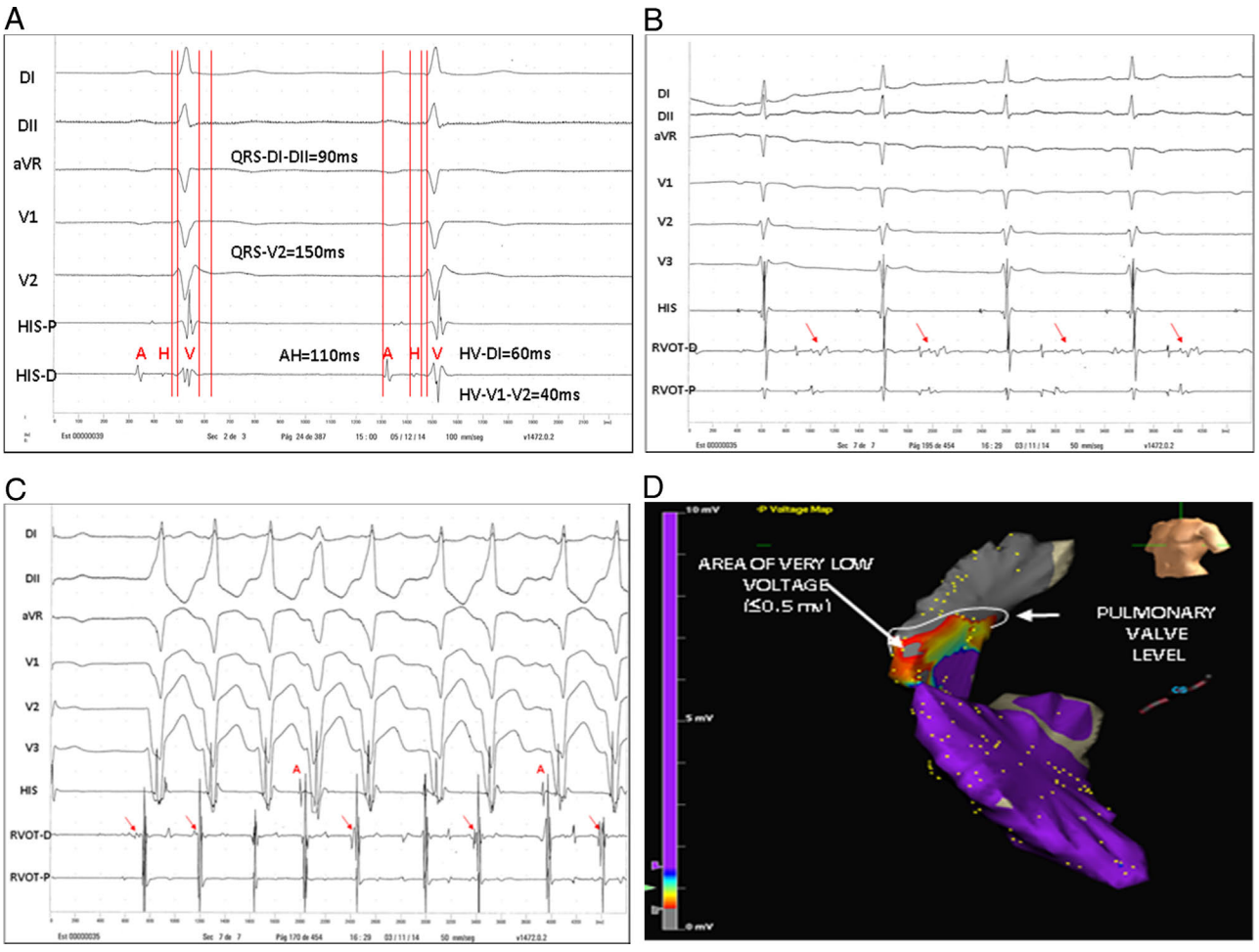

Figure 2 **A:** Baseline AH interval of 110 milliseconds, HV-DI of 60 milliseconds, and HV-V2 of 40 milliseconds; QRS duration in DII of 90 milliseconds and QRS duration in V2 of 150 milliseconds, indicating slow conduction in the right ventricular outflow tract (RVOT). **B:** Note the presence of middiastolic electrograms (EGMs) during sinus rhythm (red arrows). We identified areas that contained low-amplitude late potentials, corresponding to the anterior area of the high RVOT on the voltage map, where a systolic low-voltage EGM can also be seen in the proximal ablator. **C:** Spontaneous ventricular tachycardia from the RVOT and diastolic EGMs preceding the onset of the QRS complex can be seen (red arrows), which correspond to presystolic Purkinje-type potentials of low amplitude and high frequency preceding the QRS for 20 or 30 milliseconds. **D.** Voltage and electroanatomical maps, and the 3 areas of different voltage. HV-DI = HV interval measured DI; HV-V2 = HV interval measured V2; RVOT-D = distal right ventricular outflow tract; RVOT-P = proximal right ventricular outflow tract.

very fractionated. Fractionated EGMs probably caused by electrical activation of small bundles of tissue are a common manifestation of increased coupling resistance following separation of myocardial fibers in the reentrant circuit. In the present study, using electroanatomic mapping, voltage mapping, and conventional bipolar electrophysiological mapping of the endocardium, we observed regions of unfractionated systolic EGMs of low voltage in the RVOT, in agreement with the previous report. However, we also recorded fractionated middiastolic potentials of low voltage in the endocardium and presystolic Purkinje-type potentials, as shown in Figures 2B and 2C, which were targeted for ablation. The middiastolic potentials probably correspond to depolarization of isthmuses or channels proximal to the exit during electrical diastole, and the presystolic potentials may correspond to phenomena of spontaneous depolarization of some Purkinje cells or diseased cells of the myocardium, or activity from reentry-circuit exit regions. Spatial electrical heterogeneity within the myocardium through different genetically determined changes of diastolic potential explains high electrical instability in these patients.[7] Using TEM to observe differences in comparison to the normal zone, we found specific changes consisting of cytoplasmic degeneration of myocytes, mitochondrial swelling, and vacuolization, with cell damage and death progressively increasing from a peripheral area (0.5–1.5 mV) to a central very low-voltage area (<0.5 mV) (Figure 3). Our findings suggest that the functional alterations are correlated with ultrastructural changes. In this case, we detected no fat replacement—typical of arrhythmogenic right ventricular cardiomyopathy—no active lymphocytic myocarditis, and no Chagas myocarditis; these entities may mimic the clinical findings and ECG of BS.[8] In our patient, who had some mutations in the cardiac sodium channel, the TEM analysis did not reveal apoptotic bodies, although apoptosis is a pathogenic mechanism demonstrated in arrhythmogenic

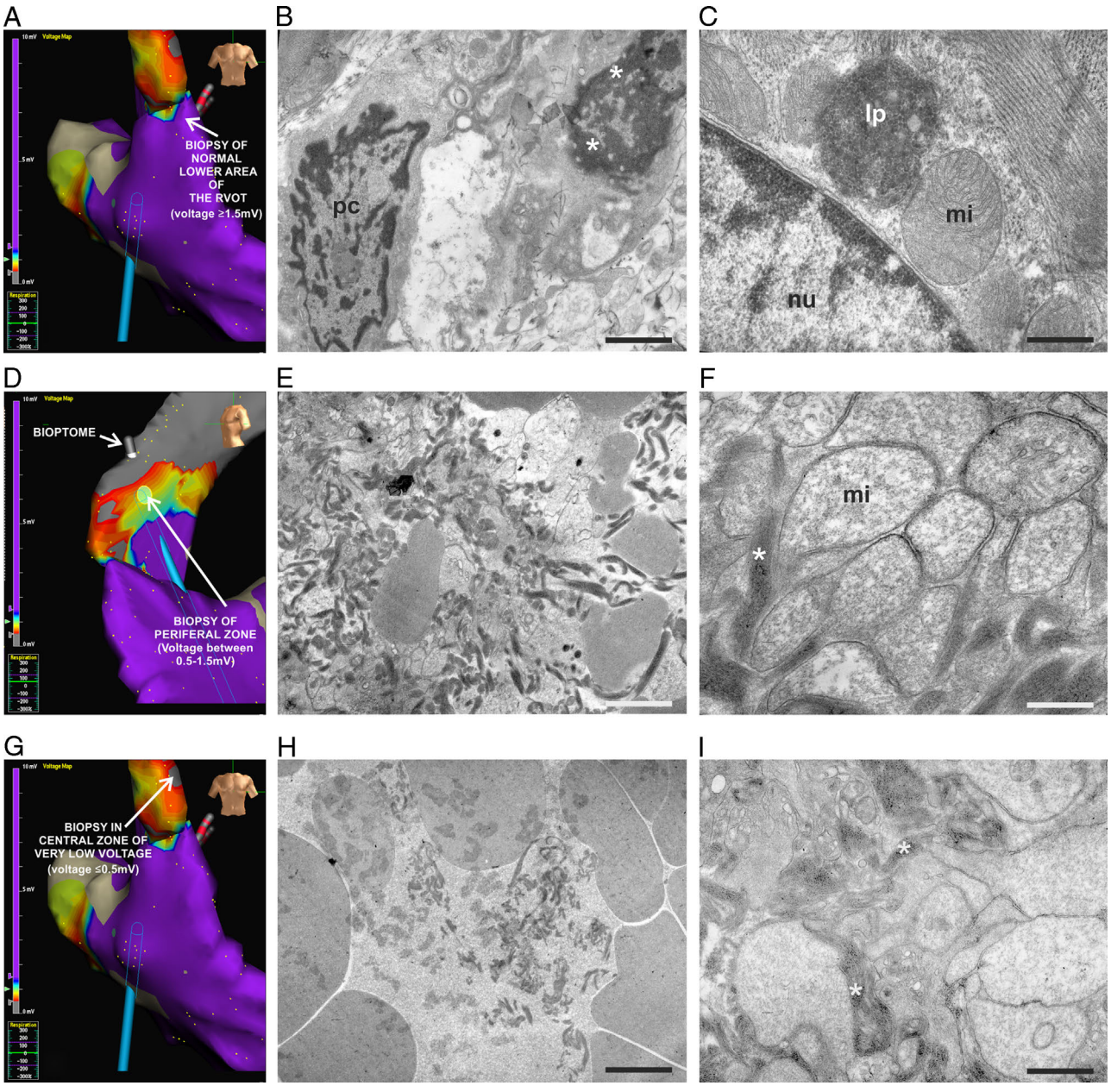

Figure 3 Endocardial biopsy by transmission electron microscopy. Voltage and electroanatomical map of **A**: normal lower area of the right ventricular outflow tract (voltage ≥ 1.5 mv), and **B:** Purkinje cell with abundant secretory vesicles in the normal lower area. Note that when approaching the pathological area, cytoplasmic disorganization, vacuolization (*) and myofibrillar remains in the adjacent cells were evident. **C:** Mitochondria showing normal crest, lipofuscin deposits near the myocyte nucleus and myofibrils with classic characteristics in normal lower area. **D**: Voltage and electroanatomical map of peripheral area (voltage between 0.5 and 1.5 mv). **E:** Myofibrillar and cellular remains in the peripheral area. **F:** Note the disappearance of the mitochondrial crests, mitochondrial swelling, and myofibrillar disorganization (*) in the same area. **G**: Voltage and electroanatomical map of central area (voltage ≤ 0.5 mv). Note the bioptome connected to the navigation system. **H:** Strong vacuolization and cell destruction in the central area. **I:** Intense cytoplasmic disorganization, vacuolization, and remains of myocardial fibers (*) in the central area. lp = lipofuscin deposits; mi = mitochondria; mf = myofibrils; nu = nucleus; pc = Purkinje cell. Scale bar: **B** 2.2 μm; **C, F, I:** 1.42 μm; **E, H:** 3.33 μm.

right ventricular cardiomyopathy, BS, and dilated cardiomyopathy.[9,10] Interestingly, an ultrastructural study showed mitochondrial swelling and loss of the crest (Figure 3). This finding raises the possibility that complete loss of mitochondrial energy does not favor the development of apoptosis but may lead to necrosis[11] and to progressive tissue damage. Heart function is highly dependent on oxidative energy generated in mitochondria, primarily by fatty acid β-oxidation, respiratory electron chain reactions, and oxidative phosphorylation. Defects in mitochondrial structure and function have been found in association with cardiovascular diseases such as dilated and hypertrophic cardiomyopathy, cardiac conduction defects and sudden death, and ischemic and alcoholic cardiomyopathy, as well as myocarditis. Whereas a subset of these mitochondrial abnormalities has a defined genetic alteration, others have not yet been

characterized.[11] Although no genetic analysis was conducted in this study, the ultrastructural results with the functional data suggest that we are in the presence of BS.

An arrhythmic event may occur when a sufficient degree of cell damage has been reached and resting potentials are reduced, through a reentrant microcircuit or triggered activity from cells that are damaged but have not yet died, which in turn would explain the presence of diastolic EGMs, such as those found in the area of peripheral lesion in this patient (Figure 3). If resting potentials reach the threshold of vulnerable epicardial potential, they could initiate a phenomenon of phase 2 reentry, whose existence was previously demonstrated.[12] We found Purkinje fibers during the TEM analysis, and some studies have shown that these fibers may be involved in the genesis of early-onset PVCs, which can trigger VT or VF.[7] These assumptions need to be investigated.

Another aspect to consider is the correlation between higher ST elevation in the upper right precordial leads during the flecainide test (second ICS) and the location of the area of low voltage in the anterior aspect of the high RVOT, as can be seen in the voltage map. We have observed this correlation in other patients (unpublished data) in whom the highest elevation of the ST segment was in the lower right leads (fourth ICS), coinciding with the anterior region of the RVOT in the voltage map. This suggests the ability of an ECG to locate the area of low voltage.

Continuing with the analysis of the baseline ECG, our patient presented an end-QRS slur with descending ST segment in the DI lead and horizontal in the aVL lead, which corresponds to an early repolarization, according to the latest consensus.[13] The changing end-QRS slur in DI and aVL leads, by "s" waves during the flecainide test, which mainly corresponds to the vector 4° depolarization of the right ventricle and RVOT, may be the expression of a higher right end conduction delay on the lateral aspect of the RVOT that is coincident with an R wave in aVR of 3 mm. Some researchers have suggested that early repolarization with a horizontal or downward-sloping ST segment is potentially more serious, since most of the cases with idiopathic VF are associated with this pattern. There is a consensus that the pattern of end-QRS notching and slurring may, on occasion, be due to late depolarization rather than early repolarization, suggesting that the term "early repolarization" should be replaced by "J waves." In the case we report, the slur or "J wave" could correspond to a delay of the depolarization in the lateral aspect of the RVOT by slow driving, since the area of the lesion extended to that place, as shown in Figure 3. If so, it could be speculated that an early repolarization with a patent type 1 or type 2 ECG of BS suggests the existence of an area of more extensive injury in the RVOT and increased arrhythmic risk.

Similar to those that have already been reported in other studies, depolarization abnormalities were present in this case; we observed a prolonged PR interval, prolonged QRS width (120 milliseconds), high R wave in aVR, and increased duration of the P wave.[14] Whereas some researchers who conducted functional studies argue the existence of a superior bundle of the right branch to the RVOT, which would be affected in BS and likely responsible for the alteration of depolarization, which was called "right end conduction delay" or "right superior fascicular block," [14] others denied its existence.[15] Interestingly, as shown in Figure 3, we found Purkinje cells in the normal region of the RVOT. In concordance with this finding, an ECG pattern recorded during a flecainide test corresponding to a right end conduction delay has been shown in Figure 1. Based on this fact, it is necessary to ask about the role of Purkinje cells in the conduction delay in the RVOT.

Conclusion

To our knowledge these findings provide the first evidence of an association between ultrastructural and functional alterations in the RVOT in BS and offer a rational approach for ablation of this substrate.

References

1. Brugada P, Brugada J. Right bundle branch block, persistent ST segment elevation and sudden cardiac death: A distinct clinical and electrocardiographic syndrome: A multicenter report. J Am Coll Cardiol 1992;20(6):1391–1396.
2. Bayés De Luna A, Brugada, Baranchuk A, Borggrefe M, et al. Current electrocardiographic criteria for diagnosis of Brugada pattern: A consensus report [published correction appears in J Electrocardiol 2013;46(1):76]. J Electrocardiol 2012;45(5):433–442.
3. Zhang J, Sacher F, Hoffmayer K, et al. Cardiac electrophysiological substrate underlying the ECG phenotype and electrogram abnormalities in Brugada syndrome patients. Circulation 2015;131(22):1950–1959.
4. Frustaci A, Priori SG, Pieroni M, Chimenti C, Napolitano C, Rivolta I, Sanna T, Bellocci F, Russo MA. Cardiac histological substrate in patients with clinical phenotype of Brugada syndrome. Circulation 2005;112(24):3680–3687.
5. Sánchez SS, Genta SB, Aybar MJ, Honoré SM, Villecco EI, Sánchez Riera AN. Changes in the expression of small intestine extracellular matrix proteins in streptozotocin-induced diabetic rats. Cell Biol Int 2000;24(12):881–888.
6. Nademanee K, Veerakul G, Chandanamattha P, Chaothawee L, Ariyachaipanich A, Jirasirirojanakorn K, Likittanasombat K, Bhuripanyo K, Ngarmukos T. Prevention of ventricular fibrillation episodes in Brugada syndrome by catheter ablation over the anterior right ventricular outflow tract epicardium. Circulation 2011;123(12):1270–1279.
7. Natale A, Raviele A, Al-Ahmad A, et al. Venice Chart International Consensus document on ventricular tachycardia/ventricular fibrillation ablation. J Cardiovasc Electrophysiol 2010;21(3):339–379.
8. Corrado D, Basso C, Buja G, Nava A, Rossi L, Thiene G. Right bundle branch block, right precordial ST-segment elevation, and sudden death in young people. Circulation 2001;103(5):710–717.
9. McNair WP, Ku L, Taylor MR, Fain PR, Dao D, Wolfel E, Mestroni L, Familial Cardiomyopathy Registry Research Group. *SCN5A* mutation associated with dilated cardiomyopathy, conduction disorder, and arrhythmia. Circulation 2004;110(15):2163–2167.
10. Valente M, Calabrese F, Thiene G, Angelini A, Basso C, Nava A, Rossi L. In vivo evidence of apoptosis in arrhythmogenic right ventricular cardiomyopathy. Am J Pathol 1998;152(2):479–484.
11. Marín-García J, Goldenthal M. The mitochondrial organelle and the heart [in Spanish]. Rev Esp Cardiol 2002;55(12):1293–1310.
12. Antzelevitch C. Brugada syndrome. Pacing Clin Electrophysiol 2006;29(10):1130–1159.
13. Macfarlane P, Antzelevitch C, Haissaguerre M, Huikuri H, Potse M, Rosso R, Sacher F, Tikkanen J, Wellens H, Yan G-X. The early repolarization pattern. A consensus paper. J Am Coll Cardiol 2015;66(4):470–477.
14. *Value of Electrocardiogram and Vectorcardiogram in the Diagnosis and Prognosis of Brugada Syndrome…20 Years Later*. In: Perez Riera AR, ed. Minneapolis, MN: St. Jude Medical; 2012.
15. Elizari MV, Raúl Levi R, Acunzo RS, Chiale PA, Civetta MM, Ferreiro M, Sicouri S. Abnormal expression of cardiac neural crest cells in heart development: A different hypothesis for the etiopathogenesis of Brugada syndrome. Heart Rhythm 2007;4(3):359–365.